Counterflow Model for Agent-Based Simulation of Crowd Dynamics

Simo Heliövaara[a,*], Timo Korhonen[b], Simo Hostikka[b], Harri Ehtamo[a]

[a] *Systems Analysis Laboratory, Aalto University, P.O. Box 11100, FI-00076 Aalto, Finland*
[b] *VTT Technical Research Centre of Finland, P.O. Box 1000, FI-02044 VTT, Finland*

Abstract

Agent-based crowd models describe pedestrians as autonomous interacting agents. Current models take into account the physical contact forces occurring in a crowd, but the description of many behavioural actions is still a challenge. This paper presents a model for agents' behaviour in counterflow situations, where they try to avoid collisions with oncoming agents. In the model, the agents observe the walking directions of the agents in front of them and choose their own actions accordingly. We implement the model to the widely used social force model, which describes the the motion of each agent in a Newtonian manner. Nevertheless, the basic idea of the counterflow model can be used with various modelling platforms. We study the effects of the model's parameters with Monte Carlo simulations and justify our selection of their values. Simulation results are compared with previously published experimental data and the results match well.

Keywords: evacuation, counterflow, FDS+Evac, crowd dynamics

*Corresponding author, Tel.: +358 50 545 8283
Email address: simo.heliovaara@hut.fi (Simo Heliövaara)

Nomenclature

Variables and Parameters of the Social Force Model

$m_i =$	mass of agent i
$\mathbf{x}_i(t)$	position of agent i
$\mathbf{v}_i(t)$	velocity of agent i
$\mathbf{v}_i^0(t)$	desired velocity of agent i
$v_i(t)$	speed of agent i
$\boldsymbol{\xi}_i(t)$	random fluctuation force on agent i
τ_i	relaxation time parameter
$\mathbf{f}_i$	total force on agent i
$\mathbf{f}_{ij}^{\text{soc}}$	social force from agent j on agent i
$\mathbf{f}_{iw}^{\text{soc}}$	social force from the walls on agent i
$\mathbf{f}_{ij}^{\text{c}}$	contact force from agent j on agent i
$\mathbf{f}_{iw}^{\text{c}}$	contact force from the walls on agent i
A_i	social force strength parameter
B_i	social force extent parameter
λ_i	anisotropy parameter of the social force
d_{ij}	distance between the centres of the circles of agents i and j which are closest to each other
r_{ij}	sum of the radii of the circles of agents i and j which are closest to each other
φ_{ij}	the angle between $\mathbf{v}_i(t)$ and the direction from agent i to agent j
Δv_{ij}^t	the difference of the tangential velocities of agents i and j when in contact
Δv_{ij}^n	the difference of their normal velocities of agents i and j when in contact
$\mathbf{t}_{ij}$	unit tangential vector of the contacting circles of agents i and j
k_{ij}	strength parameter for radial elastic force between agents i and j
κ_{ij}	strength parameter for frictional force between agents i and j
c_d	damping parameter for contact forces
I_i^z	moment of inertia on agent i
$\eta_i^z(t)$	random fluctuation torque
$M_i^z(t)$	total torque exerted on agent i by its surroundings
M_i^c	torque of the contact forces on agent i
M_i^{soc}	torque of the social forces on agent i
M_i^τ	torque of the motive force on agent i
$\mathbf{R}_i^c$	radial vector, which points from the centre of agent i to the point of contact
$\mathbf{R}_i^{soc}$	radial vector, which points from the centre of agent i to the fictitious contact point of the social force

ω^0	maximum target angular velocity of agent i
$\tilde{\omega}_i^0(t)$	target angular velocity of agent i
$\omega_i(t)$	the angular velocity of agent i
$\varphi_i(t)$	rotational angle of agent i at time t
φ_i^0	target angle of agent i, i.e., the direction of vector $\mathbf{v}_i^0$

Variables and Parameters of the Counterflow Model

$\mathbf{u}_i^0$	vector pointing to the preferred moving direction of agent i
$\mathbf{u}_i^{-\theta}$, $\mathbf{u}_i^{+\theta}$	vectors pointing angle θ to the left and right from vector $\mathbf{u}_i^0$ respectively
$S_i^{-\theta}, S_i^0, S_i^{+\theta}$	left, straight, and right sectors of the counterflow model
$S_{i,\uparrow\uparrow}^{\theta}$	the set of the non-counterflow agents in sector S_i^{θ}
$S_{i,\downarrow\uparrow}^{\theta}$	the set of the counterflow agents in sector S_i^{θ}
D_{ij}	skin to skin distance between agents i and j
$\delta_{\text{condition}}$	a binary variable that has value 1 if the condition in the subscript is true and value 0 otherwise
c_{df}	parameter for preferring agents with same direction, constant factor
d_{df}	parameter for preferring agents with same direction, speed factor
c_{cf}	parameter for avoiding agents with opposite direction, constant factor
d_{cf}	parameter for avoiding agents with opposite direction, speed factor
$c_{1\text{w}}$	parameter for avoiding directions towards walls
$c_{2\text{w}}$	parameter for avoiding sectors that are mostly inside walls
c_{v_0}	parameter for preferring straight ahead + right sectors in counterflow
d_{v_0}	parameter for preferring $\mathbf{v}_i^0$ if no counterflow, constant factor
c_{ncf}	parameter for preferring $\mathbf{v}_i^0$ if no counterflow, speed factor
$a_{\text{min,cf}}$	If counterflow, minimum social force strength
$b_{\text{min,cf}}$	If counterflow, minimum social force range
$a_{\text{w,cf}}$	parameter for decreasing social force in counterflow
c_τ	parameter for increasing motive force and torque in counterflow
τ_{min}	If counterflow, maximum motive force parameter
τ_{min}^z	If counterflow, maximum motive torque parameter

1. Introduction

Consideration of crowd dynamics is essential in the design of usable and evacuation safe venues like railway stations or passenger ships. Modelling and numerical simulations are one of the few means to rationally assess these properties. In the agent-based modelling approach, pedestrians are described as autonomous,

interacting agents, which enables the modelling of pedestrians' behaviour. Pedestrian counterflow situations occur constantly when large amounts of people move in public venues or on sidewalks. In evacuation situations, people are usually moving to the same direction and counterflow situations are not as common. Nevertheless, some occupants may try to move against the evacuation stream, e.g., to find their families or to evacuate through a different route [1, 2]. Also, as occupants try to exit a burning building, fire fighters and other emergency staff try to enter it causing counterflow.

Many of the previous approaches to describe pedestrian trail formation have been based on the idea that they leave virtual traces along their path which then attract the other pedestrians just like in the formation of ant trail systems. In the context of the social force model this approach has been called the active walker model [3]. In the cellular automaton models, a similar method is called the dynamic floor field [4]. In these models, the virtual traces are able to create trails for pedestrians moving to same direction.

The active walker model is able to produce trail formation and create lines of agents heading to a same direction. However, the drawback is that in counterflow situations the agents do not attempt to avoid the oncoming traffic and unrealistic collisions occur. In some recent articles [5, 6] this issue has been approached by developing separate models for the collision avoidance of agents. The agents first observe their environment to detect potential collisions and then adjust their velocity, i.e., moving speed and direction, to avoid them. The collision avoidance has been added to the social force model either by adding a component to the *desired velocity* [5] or by adding a new force to change the agents' trajectories [6]. These models are able to produce realistic behaviour in many situations. A restriction is that the agents can only avoid collision with one agent at a time, which, especially in the case of dense crowds, may not be enough to get realistic simulations. Another restriction, when modelling counterflow, is that these approaches are totally separate from the active walker model. It is possible that simultaneous use of the collision avoidance and active walker models causes problems as the resulting forces may contradict.

In this paper, we present a new combined model, which alters the desired moving direction of the agents, taking simultaneously into account both collision avoidance and trail formation. It is applied to the crowd dynamics model of Helbing et al. [7, 8, 9, 10], although it is applicable for other crowd dynamics models as well. The objective of our agents is to select the moving direction with the largest forward flow. In this case, we consider counterflow as negative forward flow, and thus, the agents also tend to avoid directions with counterflow. Each

time the algorithm is run the agents have three options: to keep going forward, to dodge right, or to dodge left. The decision is made by observing the flow in three sectors in front of the agent and by selecting the direction in which the forward flow is maximal. Experimental studies show that in a country of right-hand road traffic, also pedestrians tend to create right-hand traffic in counterflow situations [11]. It is reasonable to assume that in countries of left-hand road traffic also the pedestrians act accordingly. We take this effect into account by setting the agents to slightly prefer dodging to right over dodging to left. Another objective of the agents is to walk towards their target exit, and thus, they will keep going forward if no significant difference in the directions occurs.

Another new feature presented in this article is agents' ability to rotate their bodies in counterflow situations. The cross-section of a human body is elliptical and the rotational position in which they walk affects the counterflow, because agents moving shoulder first occupy much less space in the walking direction. When the model of Helbing et al. is modified by describing the agents with three overlapping circles, rotational equations of motion and a desired body angle are added analogously to the translational equations of motion and the desired velocity [12, 13]. We set the agents to change their desired angle in certain counterflow situations to avoid collisions. Test simulations show that this feature has a very significant effect on the rate of the counterflow.

FDS+Evac [13, 14, 15, 16, 17, 18] is an evacuation module of the fire simulation software Fire Dynamics Simulator (FDS), version 5 [19, 20, 21, 22, 23]. The model of Helbing et al. is used for the movement of the agents, their physical interactions, and their tendency to keep some distance to the other agents. One advantage of this is that the behaviour of each agent can be altered by adjusting its individual desired moving velocity, which describes the speed and direction in which the agent attempts to move. FDS+Evac also uses the three-circle model for the cross-section of the agents [12, 13], enabling the modelling of body rotation. The counterflow model has been implemented in FDS+Evac and the simulation results of this paper are obtained using that software.

This paper is organised as follows: In the next section we describe the agents' movement model used in FDS+Evac. In Section 3 the counterflow model is presented in detail. The fourth section describes how the parameters are selected using Monte Carlo method. In Section 5 the performance of the model is analysed both qualitatively and quantitatively and its results are compared to experimental data and other approaches. Concluding comments are given in the final section.

2. Crowd Movement Model

The Helbing et al. model [7, 8, 9, 10] is used as the starting point for pedestrian movement presented in FDS+Evac. This model introduces a social force, which is used to keep reasonable distances between pedestrians and between pedestrians and walls. The model is briefly described below. For a detailed description, see the original references. For the modification of a one-circle representation of the elliptical cross sectional shape of the human body to a three-circle one, where one large circle describes the torso and two smaller ones the shoulders, see the papers by Langston et al. [12] and Korhonen et al. [13, 14, 15, 16, 17].

Pedestrians are modelled as individual agents, which are moving in horizontal planes representing the floors of buildings. The trajectories of the agents are found by solving a coupled differential equation system consisting of equation of motions for each agent. Thus, the model can be categorised to be a continuous time and space type egress model. This approach allows each agent to have its own individual properties and behavioural models. The size of each agent is represented by three circles approximating the elliptical cross sectional shape of human body just like in the Simulex programme [24, 25, 26, 27], in the MASSEgress programme [2], and in the CrowdDMX model [12, 5]. Agents experience contact forces and moments as well as psychological and motive forces and moments. The resulting equations of motions for the translational and rotational degrees of freedom are solved using the methods of dissipative particle dynamics [28].

The combination of the model of Helbing et al. and the three-circle representation of the human body is implemented in the FDS+Evac simulation software [17], which is used in the numerical simulations in this paper. The body dimensions and the unimpeded moving speeds of the default population types in FDS+Evac are shown in Table 1. The body diameters and walking speeds are, by default, drawn randomly for each generated agent from uniform distributions, whose widths are also given in the table. The body dimensions and unimpeded walking speed distributions are taken to be same as in the Simulex programme for the "Male", "Female", "Child", and "Elderly" categories. The category "Adult" is just a simple superposition of the "Male" and "Female" categories.

Each agent follows its own equation of motion:

$$m_i \frac{d^2\mathbf{x}_i(t)}{dt^2} = \mathbf{f}_i(t) + \boldsymbol{\xi}_i(t) \,, \tag{1}$$

where $\mathbf{x}_i(t)$ is the position of agent i at time t, $\mathbf{f}_i(t)$ is the force exerted on agent i by its surroundings, m_i is the mass, and the last term, $\boldsymbol{\xi}_i(t)$, is a small random fluctuation force. The velocity of agent i is given by $\mathbf{v}_i(t) = d\mathbf{x}_i/dt$.

The force on agent i consists of several components:

$$\mathbf{f}_i = \frac{m_i}{\tau_i}\left(\mathbf{v}_i^0 - \mathbf{v}_i\right) + \sum_{j\neq i}\left(\mathbf{f}_{ij}^{\mathrm{soc}} + \mathbf{f}_{ij}^{c}\right) + \sum_{w}\left(\mathbf{f}_{iw}^{\mathrm{soc}} + \mathbf{f}_{iw}^{c}\right) \ , \tag{2}$$

where the first sum describes agent–agent interactions and the sum over w describes agent–wall interactions. The first term on the right hand side describes the motive force on the agent. Each agent tries to walk with its own specific walking speed, $v_i^0 = |\mathbf{v}_i^0|$, towards an exit or some other target along the direction given by the velocity field $\mathbf{v}_i^0$. The relaxation time parameter, τ_i, sets the strength of the motive force, which makes an agent to accelerate towards its specific walking speed.

The agent–agent interaction force in eq. (2) has two parts. For the social force term, $\mathbf{f}_{ij}^{\mathrm{soc}}$, the anisotropic formula proposed by Helbing et al. [9] is used

$$\mathbf{f}_{ij}^{\mathrm{soc}} = A_i e^{-(d_{ij}-r_{ij})/B_i}\left(\lambda_i + (1-\lambda_i)\frac{1+\cos\varphi_{ij}}{2}\right)\mathbf{n}_{ij} \ , \tag{3}$$

where d_{ij} is the distance between the centres of the circles describing the agents, r_{ij} is the sum of the radii of the circles, and the vector $\mathbf{n}_{ij}$ is the unit vector pointing from agent j to agent i. In the three circle model, the circles used in eq. (3) are those circles of the two agents, which are closest to each other. The angle φ_{ij} is the angle between the direction of the motion of agent i feeling the force and the direction to agent j, which is exerting the repulsive force on agent i. The parameters A_i and B_i describe the strength and spatial extent of the force, respectively. The parameter λ_i controls the anisotropy of the social force. If $\lambda_i = 1$, then the force is symmetric and if it is $0 < \lambda_i < 1$, the force is larger in front of an agent than behind. The psychological wall–agent interaction, $\mathbf{f}_{iw}^{\mathrm{soc}}$, is treated similarly, but values A_w, B_w, and λ_w are used for the force constants and the distances are measured from the closest circle to the wall.

The physical contact force between the agents, $\mathbf{f}_{ij}^{c}$, is given by

$$\mathbf{f}_{ij}^{c} = \left(k_{ij}(r_{ij}-d_{ij}) + c_d\Delta v_{ij}^n\right)\mathbf{n}_{ij} + \kappa_{ij}(r_{ij}-d_{ij})\Delta v_{ij}^t\,\mathbf{t}_{ij} \ , \tag{4}$$

where Δv_{ij}^t is the difference of the tangential velocities of the circles in contact, Δv_{ij}^n is the difference of their normal velocities, and vector $\mathbf{t}_{ij}$ is the unit tangential vector of the contacting circles. This force applies only when the circles are in contact, i.e., $r_{ij} - d_{ij} \geq 0$. The radial elastic force strength is given by the force constant k_{ij} and the strength of the frictional force by the force constant κ_{ij}. Note,

that eq. (4) contains also a physical damping force with a damping parameter c_d that was added by Langston et al. [12]. The original model introduced by Helbing et al. did not have this force. This parameter reflects the fact that the collisions between people are not elastic. The physical wall–agent interaction, $\mathbf{f}^c_{iw}$, is treated similarly and same force constants are used.

Eqs. (1)–(4) describe the translational degrees of freedom of the agents. The rotational degrees of freedom are treated similarly, i.e., each agent has its own rotational equation of motion:

$$I_i^z \frac{d^2\varphi_i(t)}{dt^2} = M_i^z(t) + \eta_i^z(t) \,, \tag{5}$$

where $\varphi_i(t)$ is the body angle of agent i at time t, I_i^z is the moment of inertia, $\eta_i^z(t)$, is a small random fluctuation torque, and $M_i^z(t)$ is the total torque exerted on agent i by its surroundings

$$M_i^z(t) = M_i^c(t) + M_i^{\mathrm{soc}}(t) + M_i^\tau(t) \,, \tag{6}$$

where M_i^c, M_i^{soc}, and M_i^τ are the torques of the contact, social, and motive forces, respectively.

The torque of contact forces is calculated as

$$\mathbf{M}_i^c = \sum_{j \neq i} \left(\mathbf{R}_i^c \times \mathbf{f}_{ij}^c \right) \,, \tag{7}$$

where $\mathbf{R}_i^c$ is the radial vector, which points from the centre of agent i to the point of contact, see Fig. 1. In FDS+Evac, also the social forces exert torques on the agents and these are given by the formula

$$\mathbf{M}_i^{\mathrm{soc}} = \sum_{j \neq i} \left(\mathbf{R}_i^{\mathrm{soc}} \times \mathbf{f}_{ij}^{\mathrm{soc}} \right) \,, \tag{8}$$

where only the circles, which are closest to each other, are considered. The vector $\mathbf{R}_i^{\mathrm{soc}}$ points from the centre of agent i to the fictitious contact point of the social force, see Fig. 1.

Analogous to the motive force, the first term on the right hand side of eq. (2), a motive torque is defined as

$$M_i^\tau(t) = \frac{I_i^z}{\tau_i^z} \left(\frac{\varphi_i(t) - \varphi_i^0}{\pi} \omega^0 - \omega_i(t) \right) = \frac{I_i^z}{\tau_i^z} \left(\tilde{\omega}_i^0(t) - \omega_i(t) \right) \,, \tag{9}$$

where ω^0 is the maximum target angular velocity of a turning agent, $\omega_i(t) = \frac{d\varphi_i}{dt}$ is the angular velocity, $\varphi_i(t)$ is the body angle, and φ_i^0 is the target angle, i.e., the direction of vector $\mathbf{v}_i^0$. Parameter τ_i^z is the relaxation time for the motive torque and it is analogous to τ_i from equation (2). Note that the difference of the angles is defined such that it belongs to an interval $(-\pi, \pi]$. It should be noted that in equation (9) the target angular speed, $\tilde{\omega}_i^0(t)$, is not constant. Rather, as defined in the equation, it increases when the difference between the body angle $\varphi_i(t)$ and the desired body angle $\varphi_i^0(t)$ increases. [12] used a different formula for the motive torque, which had a form of a spring force. During this work, it was noticed that such force makes the agents rotate around their axis like harmonic oscillators and, thus, an angular velocity dependent torque was introduced in this work. The form of this torque was taken to be analogous to the motive force of the translational equation.

The agent movement model presented in eqs. (1)–(9) has many parameters. Some of these parameters are related to physical dimensions of humans, such as m_i and I_i^z, but many parameters are related to the chosen model. Some of these parameters are chosen to be the same as found in the literature [8, 12] and some are estimated from test simulations. The parameters of the social force were chosen such that the specific flows through doors and corridors were appropriate. The parameters of the contact forces and the rotational degrees of freedom for the three circle representation were selected mainly by trial and error in order to obtain movement that looks realistic. Monte Carlo simulations were performed to see, which are the most important model parameters and further analysis was focused on those parameters. These test simulations and the chosen model parameters are described in the FDS+Evac guide [17].

3. Counterflow Model

The original model of Helbing et al. is not well suited for situations, where there are agents going to different directions and their paths are crossing or opposite to each other. The agents do not react to the oncoming agents explicitly. There is just a small implicit action by the social forces, but this is not large enough to hinder the agents from colliding. To overcome this deficiency we present a short range counterflow model that can be added to the FDS+Evac model. In the model, the agents observe the other agents in front of them and react by choosing one of three options: to move straight on, to dodge to the right, or to dodge to the left. The agents only react to the other agents among a short range in front of them.

In the counterflow model, the area in front of agent i is divided into three overlapping sectors, $S_i^\theta = \{S_i^{-\theta}, S_i^0, S_i^{+\theta}\}$, which are pointing to the left, $\mathbf{u}_i^{-\theta}$, straight ahead, $\mathbf{u}_i^0$, and to the right, $\mathbf{u}_i^{+\theta}$, see Fig. 2. Sectors $S_i^{-\theta}$, S_i^0, $S_i^{+\theta}$ each cover a 2θ wide sector around vectors $\mathbf{u}_i^{-\theta}$, $\mathbf{u}_i^0$, $\mathbf{u}_i^{+\theta}$ respectively. Straight ahead means always the preferred direction, $\mathbf{v}_i^0$ in eq. (2), where the agent would go without the effect of the counterflow model, e.g., the direction towards an exit door. The basic idea of the counterflow model is to choose the sector with least counterflow. This is formulated as an optimisation problem, where each agent lying within a sector either increases or decreases the score of the sector depending on its location and moving velocity.

If the front sector of agent i is not empty, it selects the movement direction $\mathbf{u}_i^*$ with the highest score among the directions of the sectors, $\mathbf{U}_i^\theta = \{\mathbf{u}_i^{-\theta}, \mathbf{u}_i^0, \mathbf{u}_i^{+\theta}\}$, ten times in every second, on the average. Agent i maximises the following expression

$$\mathbf{u}_i^* = \underset{\mathbf{u}_i^\theta \in \mathbf{U}_i^\theta}{\arg\max} \left\{ \sum_{j \in S_{i,\uparrow\uparrow}^\theta} \frac{c_{\mathrm{df}} + d_{\mathrm{df}} \langle \mathbf{v}_j - \mathbf{v}_i, \mathbf{u}_i^0 \rangle}{\max(0.2, D_{ij})} - \sum_{j \in S_{i,\downarrow\uparrow}^\theta} \frac{c_{\mathrm{cf}} - d_{\mathrm{cf}} \langle \mathbf{v}_j, \mathbf{u}_i^0 \rangle}{\max(0.2, D_{ij})} + \right.$$
$$\left. + c_{v_0} \left(\delta_{\theta>0} - \delta_{\theta<0}\right) + |c_{v_0}| v_i \delta_{\theta=0} + N_0 (c_{\mathrm{ncf}} + d_{v_0} v_i) \delta_{\theta=0} \delta_{N_0^{\mathrm{cf}}=0} \right\} , \quad (10)$$

where $\mathbf{u}_i^0 = \mathbf{v}_i^0 / |\mathbf{v}_i^0|$ is the original direction towards the target door of agent i. D_{ij} is the skin-skin distance between the agents j and i, and $\mathbf{v}_j$ and $\mathbf{v}_i$ are their velocities. The speed of agent i is denoted by $v_i = \mathbf{v}_i^0 / |\mathbf{v}_i^0|$. The angle brackets express inner products of the arguments and c_{df}, d_{df}, c_{cf}, and d_{cf} are constants. The maxima in the denominators are used to avoid divisions by zero. The agents inside the sectors S_i^θ are divided to counterflow ($\downarrow\uparrow$) and non-counterflow ($\uparrow\uparrow$) agents by projecting their desired moving direction, $\mathbf{u}_j^0$, along the desired moving direction of the current agent, $\mathbf{u}_i^0$. The symbol $\delta_{\theta>0}$ is equal to one if $\theta > 0$ and zero otherwise and similarly for the other ones.

There are terms in the above maximisation problem that prefer the right (and straight ahead) to the left to produce observed right handed traffic [11]. The right (left) sector gets an additional weight c_{v_0} ($-c_{v_0}$) and the front sector a weight $|c_{v_0}| v_i$. Note, that by giving a negative value for the parameter c_{v_0} one could prefer the left to the right. If there are no counterflow agents inside the front sector, $N_0^{\mathrm{cf}} = 0$, then this sector is preferred by a term $N_0(c_{\mathrm{ncf}} + d_{v_0} v_i)$, where c_{ncf} and d_{v_0} are constants and the number of agents in the front sector is N_0. Without this term the agents

could start to move sideways around the end of a queue at a door, which seems not a realistic behaviour.

Equation (10) describes the avoidance of counterflow agents in the absence of walls. If a sector touches a wall then some additional relatively large negative weights are given to that sector using parameters $c_{1\mathrm{w}}$ and $c_{2\mathrm{w}}$. The first parameter is used to give a negative weight that depends on the agent speed and the distance to the wall measured along the direction of the sector, $\mathbf{u}_i^\theta$. Sectors with walls are disliked more when the agent moves fast and the closer a wall is the more negative weight is given to that sector. The second parameter is used to give a large negative weight for a sector which is more or less totally inside a wall, i.e., the agent is already as close to that wall as it can be.

The social force parameters A_i, A_w, B_i, and the motive force parameters τ_i and τ_i^ζ in eqs. (2), (3), and (9) are changed when an agent faces strong counterflow and the speed of the agent is slow, as it usually is in such situations. The social force strength is reduced by a factor $a_{\mathrm{min,cf}}$ ($a_{\mathrm{w,cf}}$ for walls) at most and the range of the social force is reduced by a factor $b_{\mathrm{min,cf}}$ at most. This allows higher densities for counterflow situations. Reducing the agent-wall social force takes into account the behaviour that one is willing to move closer to walls when bypassing other people. The translational and rotational motive forces are increased by reducing the relaxation time constants by a factor c_τ up to τ_{min} and $\tau_{\mathrm{min}}^\zeta$ at most, respectively. At the same time, the target motive angle of the body is also changed so that the agent tries to move shoulder first. Similar rotation of the body angle is done if the agent is close to a wall and it finds it difficult to move ahead.

The presented counterflow model is designed for dense crowds and thus, the extents of the sectors are not very large. The range of the sectors extends maximally to three metres ahead of an agent and on the sides the sectors extend up to 1.5 m. If the speed of the agent is low then the maximal range straight ahead is approaching 1.5 m and the sectors form a semi circle as the angle of the sectors, θ, is increased from 40 degrees to 45 degrees, when the speed goes towards zero. The origin of the sectors, the point P in Fig. 2, is little bit in front the torso circle if the agent is moving freely and it is moved continuously to little bit behind the torso circle when the walking speed goes towards zero. This shift is at most $\pm R_d$, see Table 1. It is important to include the agents at the sides to the optimization problem, when the speed is low. When the speed is large the agent looks more forward and the agents at the sides are considered already to be bypassed.

The counterflow model is intended for modelling the macro-level phenomena occurring in multidirectional flows of dense crowds. Like any simulation method, the model includes some limitations and simplifications compared to the

real world. The presented counterflow model is a general method that can be applied to model multi-directional flows in any continuous pedestrian simulation model. In this paper, we have implemented it to the FDS+Evac simulation software, which uses the popular social force model for the movement of individuals. FDS+Evac enables the use different agent types which have different individual parameters like moving velocity and body dimensions. The agent types include, e.g., elders, children, male, and female. It is also possible to adjust the shape of the agents to describe different types of agents, e.g., firefighters carrying equipment and tools.

The limitations of the model include the rather short range among which agents react to others. The used range is suitable for modeling dense crowds but may produce somewhat unrealistic trajectories in sparse situations, e.g., two agents moving head-to-head in an open space. However, also in sparse open spaces, this simple short range model is able to prevent collisions in most cases, and thus, produces rather realistic flows. In our validation simulations we noticed that, with this three-sector modeling approach, the maximal range for the interaction was the 3 m, which we use in the model. Longer ranges start to produce unrealistic results. Hence, for longer range interactions and realistic trajectories in sparse populations, a completely different modeling approach would be needed.

Also the approach of modeling agents in two dimensions is a simplification of the real world situation. On a plane, it is not possible to consider the effect of agents' different heights on the dynamics, which might be significant, e.g., in a crowd where adults and children are mixed together. Modeling only two dimensions is a simplification that is made by almost all current pedestrian simulation models because adding the third dimension would make the models much more complicated and computationally heavy.

4. Parameter Selection

Many different methods were used to analyse the effects of the parameters of the counterflow model and to select their values. The values of some parameters were found by trial-and-error to avoid unrealistic movement. For the cases, where all agents were mainly going towards the same direction, results were expected to be close to those obtained with older versions of the programme as they have been validated before. The effect of some other parameters on the simulation results was carefully investigated.

Monte Carlo simulations were performed to see which parameters of the counterflow model have significant effect on the results. Four different geometries were

used in the Monte Carlo simulations. A door geometry shown on the left in Fig. 5 with 1 m and 2 m wide doors was used to study the behaviour of the model when there is no counterflow. There were 100 agents randomly located in the 5 m $\times$ 5 m square in front of the door. To test the model in counterflow, the IMO test case 8 geometry [29] was used. In this test, there are two 100 square metre rooms connected by a 2 m wide and 10 m long corridor. Both rooms were initially populated by 100 agents. In addition, a 4 m wide corridor was used to see how the model worked when there was more space for the agents to pass each other. The monitored output quantity was the specific flow in the door geometries and for the corridor cases the entering time of the last agent from the left room to the right room was detected. The Spearman's rank correlation coefficients (RCC) were calculated for these four cases and they are shown in Fig. 3. Total of one thousand egress simulations with different random initial properties were performed for each of these four cases. The default "Adult" agent type of FDS+Evac was used in the calculations, but in total fifteen different parameters of the counterflow model were varied.

The most important parameters, according to the Monte Carlo simulations, were examined further with studies, where different parameters were varied separately and hundred simulations were performed for each discretely chosen value of the parameters. The geometries used in these studies were the 2 m wide corridor geometry and the door geometry with 1 m and 2 m wide doors.

The results of the parametric studies are shown in Fig. 4, where the error bars are showing the standard deviation of the hundred simulations performed for each discrete value of the parameters. It can be seen that the counterflow model does not affect the flows through doors much if reasonable parameter values are used. This is a good result, because the intention was not to change the flows through doors in situations, where there is no counterflow. There is some variation of the results for the counterflow test case when the different parameters are varied, but these variations are not generally large.

Based on the above mentioned simulations, the default values for the parameters of the counterflow model were specified, see Table 2. These parameter values are not necessarily optimal for counterflow, but they produce reasonable results without ruining the non-counterflow properties of the model. Also, the above mentioned tests showed that the simulation results are not sensitive to the exact values of the parameters of the counterflow model.

5. Model Validation

Two of the most important factors affecting the outcomes of evacuations and evacuation simulations are the speed in which a crowd is able to pass an exit and the effect of crowd density on pedestrians' walking speed. The FDS+Evac model has been previously found to produce realistic flows in both cases. In this paper we add a new feature, the counterflow model, to the FDS+Evac and it is important make sure that the fundamental results of the model are not affected. In Sections 5.1 and 5.2 we study the effect of implementing the counterflow model on the corridor flows and door flows produced by FDS+Evac.

In Sections 5.3, 5.4, and 5.5, we present simulation results from different test cases with multi-directional flows.

5.1. Flows in Corridors

In the research of pedestrian flows, the dependence of the specific crowd flow rate on the crowd density is generally called the "fundamental diagram". It shows how the specific flow first increases when the crowd density is increased, but then starts to decrease as the density becomes high enough to hinder the walking. In the first test case, the specific flow rates calculated by FDS+Evac are compared to experimental results on horizontal floors using the geometry shown in Fig. 5. The corridor is modelled as a loop to avoid the effects of inflow and outflow boundary conditions.

In Fig. 6, the predicted specific flow rates (lines with markers) are compared against some experimental specific flow rates obtained for pedestrian traffic flows (markers). The experimental results are extracted from Daamen [30] and the references are given there. Also the SFPE Handbook [31] engineering values are shown in the figure as a black line. The FDS+Evac simulations were performed with two different parameter sets, label "default" refers to the default agent type "Adult" of FDS+Evac and label "fast" refers to an otherwise same parameter set, but $\lambda_i = 0.5$ is used for the anisotropy parameter of the social force, see eq. (3). It is seen that the FDS+Evac predictions for specific human flows lie within the experimental values. The FDS+Evac predictions with default parameters are quite close to the SFPE Handbook values, whereas the other tested parameter set produces somewhat larger flows.

5.2. Flows through Doors

The geometry used in Sec. 4 for parameter sensitivity studies was also used to study the flows through doors, see the left hand side of Fig. 5. In Fig. 7, the predic-

tions of FDS+Evac model for specific flows through doors are compared to simulation programmes Simulex [24, 25, 26, 27] and MASSEgress [2]. The results of MASSEgress ("MASSEgress") and Simulex ("Simulex, Pan") are extracted from Pan [2], where Simulex version 11.1.3 from year 1998 was used. Shown are also results calculated by the authors using Simulex version 2009.1.0.3 ("Simulex, VTT"), where the standard Simulex person type "Office Staff" was used and the exit was about 2.5 m behind the hole describing the door. This way the agents are not taken away from the calculation at the door line and the agents queueing at the door will feel these agents. If the agents are removed right at the door then the (specific) flows could be much larger as stated in the Simulex User Guide [24]. The FDS+Evac simulations were performed with two different parameter sets, labels "Male"/"Female"/"Adult"/"Elderly" refer to the corresponding default agent types of FDS+Evac and labels "Male 2"/"Female 2"/"Adult 2"/"Elderly 2" refer to parameter sets, where value $\lambda_i = 0.5$ is used for the anisotropy parameter of the social force, see eq. (3).

It is seen that FDS+Evac is able to produce reasonable flows through doors. For some applications, the flows generated by the default parameter values may be considered too low of high, but it is quite straightforward to modify the parameters of FDS+Evac to reach specific flows that are more relevant to a specific egress case. The present default values were chosen to so that the predicted specific flows were close to the commonly used engineering values, like the SFPE Handbook values [31] and the values in IMO guidelines [29], where 1.3 persons per second per effective width is the maximum specific flow.

5.3. Counterflow in Corridors

To analyse the effect of the presented model in a counterflow situation, we ran simulations in the IMO test geometry 8 [29], where a 2 m wide corridor connects two rooms. There were 100 agents in one room and one agent in the other one. All agents were set to enter the corridor simultaneously trying to move to the other room.

When the simulation were ran without the counterflow model, the single agent got pushed out of the corridor by the crowd. As illustrated in Fig. 8, the agent collided head on with the oncoming agents and was unable to enter the corridor until the whole crowd had passed it. This result is clearly unrealistic and the need for a better model for such situations is obvious.

Using the presented counterflow model, the single agent was able to penetrate through the oncoming crowd as illustrated in Fig. 9. At first the agents dodged each other and the single agent ended up against the wall on the right hand side

of the corridor. Then the agent moved shoulder first along the wall and the crowd tried to avoid colliding with the agent.

It took about 25 seconds for the single agent to pass the corridor and the crowd. However, the time may vary from one simulation to another, as the simulation model has many stochastic variables, e.g., the agents' individual properties, their initial positions, and small random forces affecting the trajectories of the agents. Qualitatively, the actions of the agents appeared to be rather realistic in this test case.

A number of theoretical analyses have been published on pedestrian counterflow [7, 32, 33, 34], but only a few sets of data of actual experiments are available [35, 11]. Isobe et al. [35] ran experiments with university students in a 12 m by 2 m corridor. Initially, 50% of the students were randomly located in the left half of the corridor and the other 50% in the right half. As the experiment started, the students in the right half tried to walk to the left end of the corridor and vice versa. The same experiment was ran with different numbers of students to analyse the effect of population density on the flow rates.

Fig. 10 presents the results of the experiment and the simulation results of FDS+Evac with the counterflow model. In the simulations, the body dimensions and walking speeds of the agents were selected to match the properties of the students participating in the experiment. Hence, 50% of the agents were generated from FDS+Evac default type "Female", but the type "Female under 30 years" walking speeds according to IMO [29] were used. Similarly, the other 50% of the agents were the default type "Male" with "Male under 30 years" walking speeds. Fig. 10 shows that the simulation results match the experimental observations very well in all population densities.

Kretz et al. [11] ran counterflow experiments in a corridor in a slightly different setting. While there was no space in between the groups of right walkers and left walkers in the initial setting of Isobe et al., Kretz et al. had the two groups standing 20 meters apart each other. Kretz et al. also varied the relative sizes of the two opposing groups by using ratios of 50%/50%, 66%/34%, 90%/10% and 100%/0% between the sizes of the two groups. The flows measured by Kretz et al. were significantly faster than those of Isobe et al. Because both experiments were ran with university students, a likely reason for the difference is the settings of the experiments. The 20 metre gap between the groups is significant, as the test persons are able to form lanes already before the two groups encounter, and thus, the encounter is much smoother.

Simulations of FDS+Evac with the counterflow model in the setting of Kretz et al. produced flows around 35% up to 65% slower than the experimental results

as the proportion of the counterflow agents increased. The main reason for this difference is the nature of the counterflow model. Because the maximum range of the model is 3 metres, the agents are not able to react to the counterflow before they are within that range, and thus, the 20 metre empty part of the corridor is not exploited as well as in the experiment. It is not straightforward to extend the presented counterflow model to such longer ranges. If the radii of the sectors is increased, also agents that are far from a collision course with the dodging agent would start affecting its actions. The presented model is able to prevent the occurrence of unrealistic jams and it gives realistic results in dense crowds. For a perfectly realistic model for longer range collision avoidance, a different and more complicated approach would be needed.

5.4. Intersection

An intersection of two 4 m wide corridors with agents moving to all four directions was simulated. The results show that with relatively high densities the intersection gets completely blocked without the counterflow feature but is very fluent when the model is used. From the simulation snapshot of Fig. 11 it can be noticed that the agents moving to same directions tend to create lines. This is a well known phenomenon that has been observed in real crowds and modelled in several articles, see, e.g., [7, 32, 36].

A similar geometry was also simulated with the active walker model [3], which was said to sometimes produce roundabout traffic with the rotation direction changing from time to time. The roundabout traffic was observed also in our simulations. However, the rotation direction was counterclockwise and it did not change during the simulations or from one simulation to another. This is likely to be due to the agents' tendency to dodge to the right rather than to the left.

5.5. Merging Flows

Especially in high-rise buildings the behaviour of merging flows is a key factor affecting the outcome of evacuations. In fire emergencies, such buildings are evacuated through the staircases that become highly populated. Merging flows occur when evacuees try to enter a staircase where other evacuees from higher floors are already moving down. The nature of these merging streams partly dictates the order and speed in which the occupants of a building are evacuated.

Some observations of merging streams have been reported in the literature (for a thorough literature review, see [37]) but detailed understanding of the process under different circumstances does not exist. The factors affecting the merging

process include population density and the geometry in which the two streams merge.

We examined the effect of the counterflow model on merging flows in two test geometries that were originally presented by Galea et al. [37]. In the first test case, there is an exit at one end of a narrow straight corridor, where the agents are only able to move in a single line. Another equally narrow corridor merges into this corridor in a straight angle. Agents enter the system at the ends of the corridors at a rate that keeps the corridors full throughout the simulation. The geometry and setting are illustrated in Fig. 12. The goal of the agents is to move towards the exit. Hence, competition occurs in the merging area, when agents from the merging corridor try to enter the corridor heading to the exit. This setting is not an actual counterflow situation because the two flows merge in a straight angle. However, it is likely that the counterflow model will affect the simulation outcomes also in this sort of situations.

The test case was simulated in 100 test runs, each of the runs lasting until 200 agents had exited. When using FDS+Evac without the counterflow model, 57.4% of the agents that made it to the exit came from the straight corridor and 42.6% from the merging corridor. The application of the counterflow model decreased the proportion of the straight going agents to 53.5%, but the difference to the original model is not statistically significant. These results differ only slightly from the the buildingEXODUS model, which produced nearly equal flows from both corridors over a long time interval [37].

The second test case is a landing with dogleg stairs. One stream of agents approaches the landing through the stairs from the above floor, while the other stream enters the landing through a door. All of the agents are heading to the stairs to the below landing. Two different configurations were studied: In case (a), the door is adjacent to the incoming stair, while in case (b), the floor is on the opposite side of the landing. The geometries used in the test cases are described in Fig. 13.

Table 3 presents the results of the second merging flow test simulations. The simulation results of FDS+Evac were obtained from 100 test runs, each of which consisting of 400 agents reaching the landing below the merging one. The general result with all simulation models is that with the door adjacent to the incoming stairs, the door flow is equal or greater than the stair flow, as with the door opposite to the stairs, the door flow is equal or less than the stair flow. Similarly to the first merging flow test case, it appears that the results just differ slightly when using FDS+Evac with or without the counterflow model.

The effect of the door location on the landing has been studied experimentally

in similar geometries by Takeichi et al. [38]. The magnitude of the door flow to the landing was measured with the door both adjacent and opposite to the incoming stairs. Also the density of people in the stair stream was varied between 1–3 people/m^2. The experiments were ran with only 27 participants, and thus, the results may not be completely accurate for a steady state flow over a longer period. Nevertheless, the results suggest that locating the door adjacent to the incoming stairs increases the door flow rate significantly. With the density of people in the stair stream around $2.0 \sim 3.0$ people/m^2, the opposite location decreased the door flow by 15–20% compared to the adjacent location. Numerical simulations with the counterflow model resulted a decrease of 19% under similar circumstances.

Hence, the results of FDS+Evac with the counterflow model seem to match well also with these empirical results. The results with FDS+Evac are quite similar also without the counterflow model. The difference to the results of buildingEXODUS is quite significant. BuildingEXODUS is a discrete space cellular automaton based model so the difference to our results is not very surprising.

In both of the test cases of merging flows, applying the counterflow model did not significantly affect the results compared to the original FDS+Evac model. This result is natural, as the test cases are not actual counterflow situations with agents moving in opposite directions. The simulation results with FDS+Evac match the experimental data of Takeichi et al. relatively well. To obtain detailed and reliable data of the merging process in staircases, further experiments are still required.

6. Conclusions

This article presents how the FDS+Evac model for crowd dynamics [14, 13, 18] is extended to better describe counterflow situations. The model uses the equations of Helbing et al. [8, 7] to describe the physical and psychological interactions occurring in a crowd and the three-circle approach [12, 13] to model the elliptical shape of the cross-section of a human body. Without the counterflow extension, the FDS+Evac model works relatively well in situations, where all agents are trying to move to the same direction, but is found to create unrealistic jams and collisions in counterflow. We present a new approach where the agents try to avoid collisions by adjusting their walking directions and by rotating their bodies to move shoulder first. The agents are also set to increase their motive force and decrease the social force in counterflow situations to allow the other agents to come closer when passing by. In previous approaches the shoulder rotation has not been considered and the agents have only been able to dodge one other agent at a time. In our model, agents compare different walking directions and select

the one with the least counterflow. This way the agents are able to dodge multiple agents at a time, which is essential in dense crowd situations.

The original presentation of the three-circle model [12] described the rotation of the agents with a spring force, resulting unrealistic oscillation of body angles. In this paper, we reformulate the rotation equation by making the form of the motive torque analogous to the motive force of the translational equation. This results in more realistic appearing motion.

The effect of the model parameters was studied using Monte Carlo simulations and the parameter values were selected according to these results. Validation simulations were also performed in normal one directional flows through exits and corridors. We found out that the counterflow model has very little effect on these well functioning properties of the original model, which is important for its applicability.

We compared simulation results of our model to experimental data of counterflow in a corridor by Isobe et al. [35]. The simulations seemed to match the data very well in all population densities, which is rather surprising considering the simple basis of the model. Qualitative analysis of test simulations show that the avoidance actions of the agents appear to be rather realistic in both dense and sparse crowds. The implementation of the counterflow model improved the performance of FDS+Evac significantly in multi-directional flows. The model is able to prevent unrealistic jams, but it also creates behaviour in counterflow situations, where agents moving to the same direction end up walking along the same path. This lane formation phenomenon has been observed in real crowds and is modelled in several articles [7, 32, 36].

The presented modelling approach enables realistic simulation of dense crowds moving in different directions. Simulation results match experimental data very well and the modelling approach is applicable to most agent-based pedestrian models.

Acknowledgements

The development work of FDS+Evac has been funded by the VTT Technical Research Centre of Finland, the Finnish Funding Agency for Technology and Innovation, the Finnish Fire Protection Fund, the Ministry of the Environment, and the Academy of Finland.

[1] Ehtamo, H., Heliövaara, S., Korhonen, T., Hostikka, S.. Game theoretic best-response dynamics for evacuees' exit selection. Advances in Complex Systems 2010;13(1):113–134.

[2] Pan, X.. Computational modeling of human and social behaviors for emergency egress analysis. Dissertation; Stanford University; Palo Alto, CA, USA; 2006.

[3] Helbing, D., Molnár, P., Schweitzer, F.. Computer simulations of pedestrian dynamics and trail formation. In: Evolution of Natural Structures, Proceedings of the 3rd International Symposium of the SFB 230, Stuttgart. 1998, p. 229–234.

[4] Schadschneider, A., Burstedde, C., Klauck, K., Zittartz, J.. Simulation of pedestrian dynamics using a 2-dimensional cellular automaton. Physica A 2001;295:507–525.

[5] Smith, A., James, C., Jones, R., Langston, P., Lester, E., Drury, J.. Modelling contra-flow in crowd dynamics DEM simulation. Safety Science 2009;47:395–404.

[6] Pelechano, N., Allbeck, J., Badler, N.. Controlling individual agents in high-density crowd simulation. In: ACM SIGGRAPH / Eurographics Symposium on Computer Animation (SCA'07). 2007, p. 99–108.

[7] Helbing, D., Molnár, P.. Social force model for pedestrian dynamics. Physical Review E 1995;51(5):4282–4286.

[8] Helbing, D., Farkas, I., Vicsek, T.. Simulating dynamical features of escape panic. Nature 2000;407:487–490.

[9] Helbing, D., Farkas, I.J., Molnár, P., Vicsek, T.. Simulation of pedestrian crowds in normal and evacuation situations. In: Schreckenberg, M., Sharma, S.D., editors. Pedestrian and Evacuation Dynamics. Berlin: Springer; 2002, p. 21–58.

[10] Werner, T., Helbing, D.. The social force pedestrian model applied to real life scenarios. In: Galea, E.R., editor. Pedestrian and Evacuation Dynamics 2003, Proceedings of 2nd International Conference. University of Greenwich, London, UK: CMS Press; 2003, p. 17–26.

[11] Kretz, T., Grünebohm, A., Kaufman, M., Mazur, F., Schreckenberg, M.. Experimental study of pedestrian counterflow in a corridor. Journal of Statistical Mechanics: Theory and Experiment 2006;:2527–2539. P10001.

[12] Langston, P.A., Masling, R., Asmar, B.N.. Crowd dynamics discrete element multi-circle model. Safety Science 2006;44:395–417.

[13] Korhonen, T., Hostikka, S., Heliövaara, S., Ehtamo, H., Matikainen, K.. Integration of an agent based evacuation simulation and the state-of-the-art fire simulation. In: Proceedings of the 7th Asia-Oceania Symposium on Fire Science & Technology. 20-22 September, 2007, Hong Kong; 2008,.

[14] Korhonen, T., Hostikka, S., Heliövaara, S., Ehtamo, H., Matikainen, K.. FDS+Evac: evacuation module for Fire dynamics simulator. In: Proceedings of the Interflam2007: 11th International Conference on Fire Science and Engineering. London, UK: Interscience Communications Limited; 2007, p. 1443–1448.

[15] Korhonen, T., Hostikka, S., Heliövaara, S., Ehtamo, H.. FDS+Evac: Modelling social interactions in fire evacuation. In: Proceedings of the 7th International Conference on Performance-Based Codes and Fire Safety Design Methods. Bethesda, MD, USA: SFPE; 2008, p. 241–250.

[16] Korhonen, T., Hostikka, S., Heliövaara, S., Ehtamo, H.. FDS+Evac: An agent based fire evacuation model. In: Klignsch, W.W.F., Rogsch, C., Schadschneider, A., Schreckenberg, M., editors. Pedestrian and Evacuation Dynamics 2008. Springer; 2010, p. 109–120.

[17] Korhonen, T., Hostikka, S.. Fire dynamics simulator with evacuation: FDS+Evac - Technical reference and user's guide. VTT Working Papers 119; VTT Technical Research Centre of Finland; Espoo, Finland; 2009.

[18] Hostikka, S., Korhonen, T., Paloposki, T., Rinne, T., Matikainen, K., Heliövaara, S.. Development and validation of FDS+Evac for evacuation simulations, project summary report. VTT Research Notes 2421; VTT Technical Research Centre of Finland; Espoo, Finland; 2007.

[19] McGrattan, K., Hostikka, S., Floyd, J., Baum, H., Rehm, R., Mell, W., et al. Fire dynamics simulator (version 5) technical reference guide volume 1: Mathematical model. NIST Special Publication 1018-5; National Institute of Standards and Technology; Gaithersburg, MD, USA; 2009.

[20] McGrattan, K., Hostikka, S., Floyd, J., McDermott, R., Prasad, K.. Fire dynamics simulator (version 5) technical reference guide volume 3: Valida-

tion. NIST Special Publication 1018-5; National Institute of Standards and Technology; Gaithersburg, MD, USA; 2009.

[21] McGrattan, K., Klein, B., Hostikka, S., Floyd, J.. Fire dynamics simulator (version 5) user's guide. NIST Special Publication 1019-5; National Institute of Standards and Technology; Gaithersburg, MD, USA; 2009.

[22] McGrattan, K.. Fire dynamics simulator (version 5) technical reference guide volume 4: Software configuration management plan. NIST Special Publication 1018-5; National Institute of Standards and Technology; Gaithersburg, MD, USA; 2009.

[23] McDermott, R., McGrattan, K., Hostikka, S., Floyd, J.. Fire dynamics simulator (version 5) technical reference guide volume 2: Verification. NIST Special Publication 1018-5; National Institute of Standards and Technology; Gaithersburg, MD, USA; 2009.

[24] IES, . Simulex User Guide – Virtual Environment 5.8. Integrated Environmental Solutions Ltd.; Glasgow, Scotland, UK; 2009.

[25] Thompson, P.A., Marchant, E.W.. A computer model for the evacuation of large building populations. Fire Safety Journal 1995;24:131–148.

[26] Thompson, P.A., Marchant, E.W.. Testing and application of the computer model 'Simulex'. Fire Safety Journal 1995;24:149–166.

[27] Thompson, P., Lindstrom, H., Ohlsson, P., Thompson, S.. Simulex: Analysis and changes for IMO compliance. In: Galea, E.R., editor. Pedestrian and Evacuation Dynamics 2003, Proceedings of 2nd International Conference. University of Greenwich, London, UK: CMS Press; 2003, p. 173–184.

[28] Vattulainen, I., Karttunen, M., Besold, G., Polson, J.M.. Integration schemes for dissipative particle dynamics simulations: From softly interacting systems towards hybrid models. Journal of Chemical Physics 2002;116:3967–3979.

[29] IMO, . Guidelines for evacuation analyses for new and existing passenger ships. MSC/Circ. 1238; International Maritime Organization; London, UK; 2007.

[30] Daamen, W.. Modelling passenger flows in public transport facilities. Ph.D. thesis; Delft University of Technology; The Netherlands; 2004.

[31] Gwynne, S.M.V., Rosenbaum, E.R.. The SFPE handbook of fire protection engineering; chap. 3-13. Quincy, MA, USA: National fire protection association; fourth ed.; 2008,.

[32] Schadschneider, A., Burstedde, C., Kirchner, A., Klauck, K., Zittartz, J.. Cellular automaton approach to pedestrian dynamics - Applications. In: Schreckenberg, M., Sharma, S., editors. Pedestrian and Evacuation Dynamics. Springer; 2001, p. 87–97.

[33] Tajima, Y., Takimoto, K., Nagatani, T.. Pattern formation and jamming transition in pedestrian counter flow. Physica A 2002;313:709–723.

[34] Blue, V.J., Adler, J.L.. Cellular automata microsimulation for modeling bi-directional pedestrian walkways. Transportation Research Part B: Methodological 2001;35:293–312.

[35] Isobe, M., Adachi, T., Nagatani, T.. Experiment and simulation of pedestrian counter flow. Physica A 2004;336:638–650.

[36] Hoogendoorn, S.P., Daamen, W.. Pedestrian behavior at bottlenecks. Transportation Science 2005;39:147–159.

[37] Galea, E.R., Sharp, G., Lawrence, P.J.. Investigating the representation of merging behavior at the floor–stair interface in computer simulations of multi-floor building evacuations. Journal of Fire Protection Engineering 2008;18:291–316.

[38] Takeichi, N., Yoshida, Y., Sano, T., Kimura, T., Watanabe, H., Ohmiya, Y.. Characteristics of merging occupants in a staircase. Fire Safety Science 2005;8:591–598.

Table 1: Unimpeded walking velocities and body dimensions in FDS+Evac. R_s is the radius of the two shoulder circles and R_t is the radius of the torso circle. These three circles are enveloped by a larger circle, whose radius is R_d. The offset of the centres of the shoulder circles from the middle of the torso circle is given by $d_s = R_d - R_s$.

Body type	R_d (m)	R_t/R_d (-)	R_s/R_d (-)	d_s/R_d (-)	Speed (m/s)
Adult	0.255±0.035	0.5882	0.3725	0.6275	1.25±0.30
Male	0.270±0.020	0.5926	0.3704	0.6296	1.35±0.20
Female	0.240±0.020	0.5833	0.3750	0.6250	1.15±0.20
Child	0.210±0.015	0.5714	0.3333	0.6667	0.90±0.30
Elderly	0.250±0.020	0.6000	0.3600	0.6400	0.80±0.30

Table 2: The default values used for the short range counterflow model in FDS+Evac. Most of the values are dimensionless factors but the two last ones have dimensions.

Parameter	Default	Description
c_{df}	2.0	Prefer agents with same direction, constant factor
d_{df}	1.0	Prefer agents with same direction, speed factor
c_{cf}	1.0	Dislike agents with opposite direction, constant factor
d_{cf}	2.0	Dislike agents with opposite direction, speed factor
c_{1w}	5.0	Dislike directions towards walls
c_{2w}	10.0	Reject sectors that are mostly inside walls
c_{v_0}	1.0	If counterflow, prefer straight ahead + right
d_{v_0}	1.0	Prefer $\mathbf{v}_i^0$ if no counterflow, constant factor
c_{ncf}	2.0	Prefer $\mathbf{v}_i^0$ if no counterflow, speed factor
$a_{\mathrm{min,cf}}$	0.5	If counterflow, minimum social force strength
$b_{\mathrm{min,cf}}$	0.3	If counterflow, minimum social force range
$a_{\mathrm{w,cf}}$	1.0	If counterflow decrease social force
c_τ	0.25	If counterflow increase motive force and torque
τ_{min}	0.10 s	If counterflow, maximum motive force parameter
τ^z_{min}	0.05 s	If counterflow, maximum motive torque parameter

Table 3: The average proportions of the agents from the stairs and the door in the population entering the stairs to the below landing.

	Test A: Adjacent		Test B: Opposite	
	Stair Flow	Door Flow	Stair Flow	Door Flow
Original FDS+Evac	42.9%	57.1%	51.2%	48.8%
Collision Avoidance	49.6%	50.4%	59.2%	40.8%
buildingEXODUS	24.5%	75.5%	51.5%	48.5%

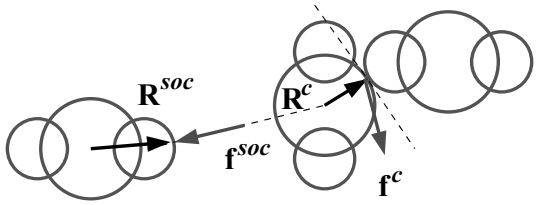

Figure 1: Definitions of the radial vectors $\mathbf{R}^c$ and $\mathbf{R}^{soc}$.

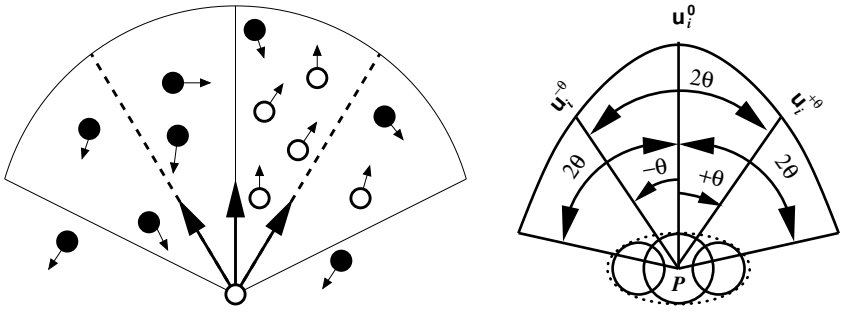

Figure 2: A sketch of the model and the definition of the sectors used in the short range counterflow model.

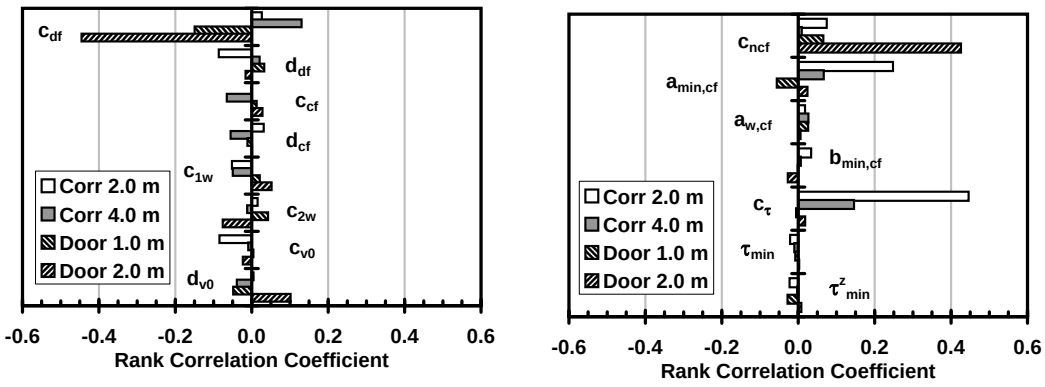

Figure 3: Rank correlation coefficients (RCC) for the emptying time through doors and corridors. Door widths 1.0 m and 2.0 m and corridor widths 2.0 m and 4.0 m were used.

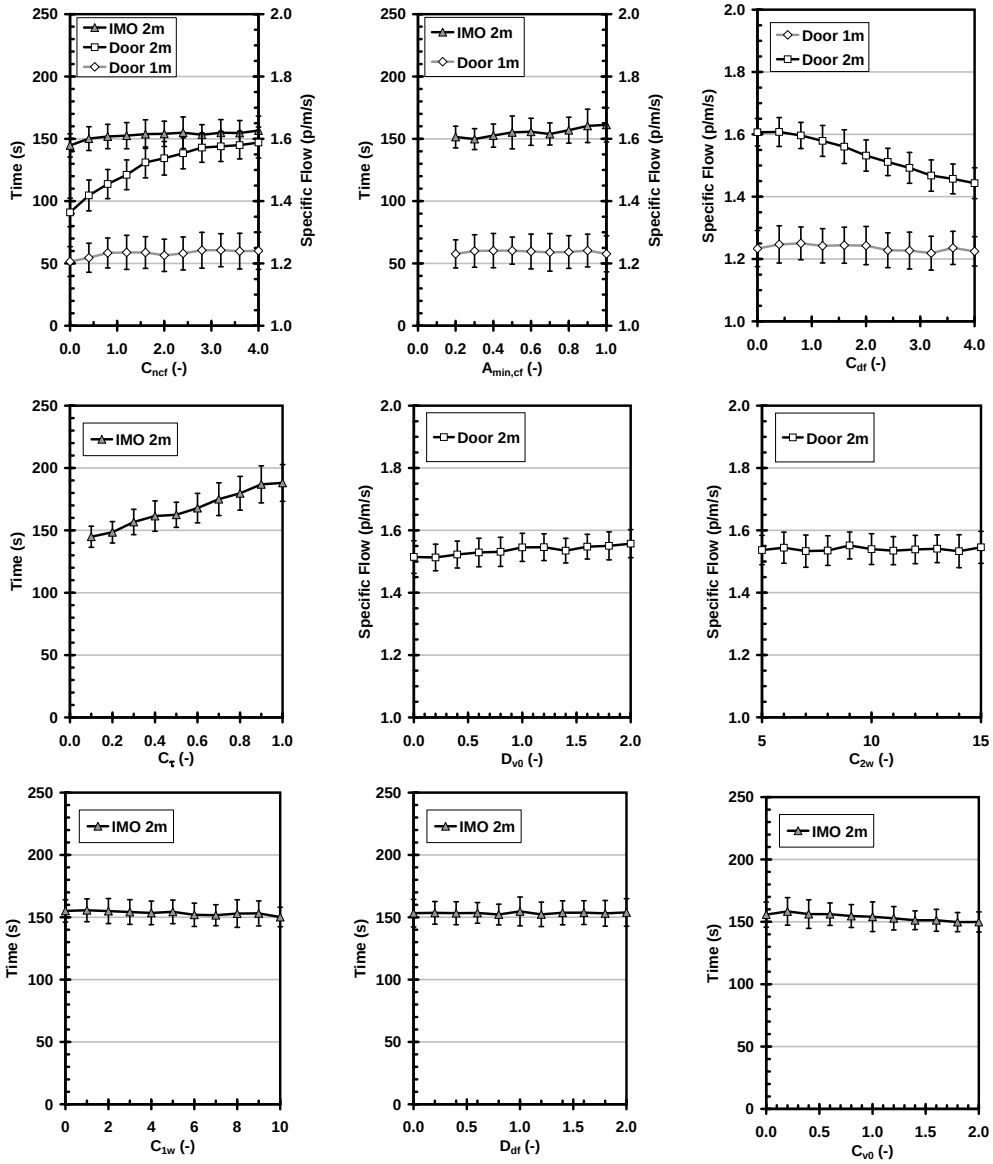

Figure 4: Effects of different counterflow model parameters on the specific flows through doors and on the emptying time of the left room for IMO test case 8. Two different doors widths, 1 m and 2 m, were used.

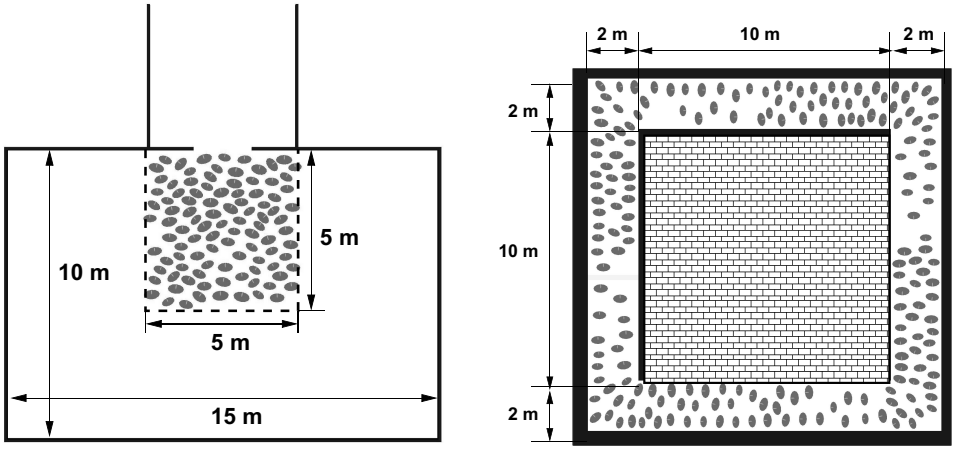

Figure 5: Test geometries used to calculate the specific flows through doors and corridors.

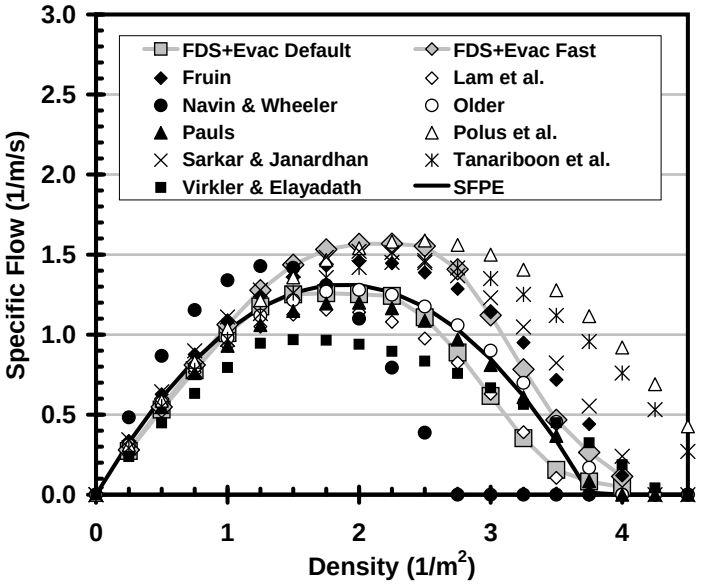

Figure 6: The specific flows in corridors.

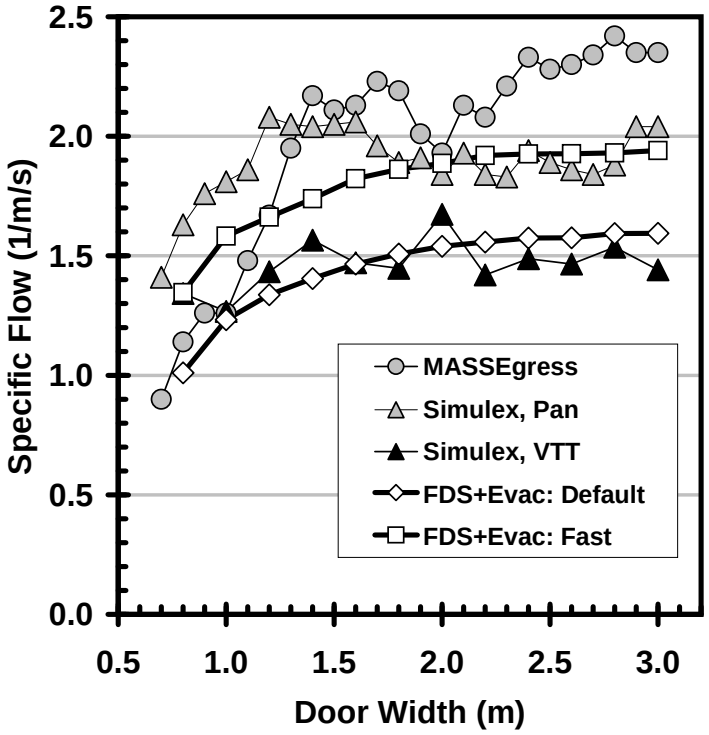

Figure 7: The specific flows through doors.

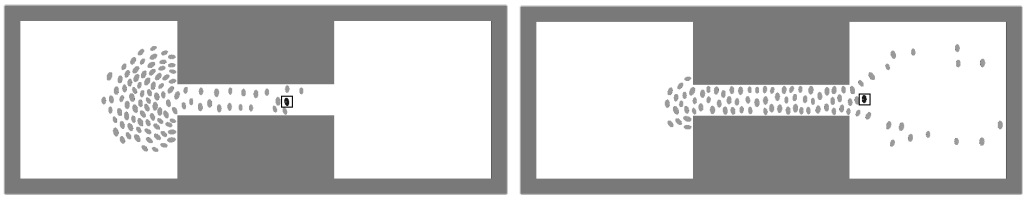

Figure 8: Snapshots of a simulation without the counterflow model. The single agent is black and highlighted with a square. The agents are unable to avoid collisions and the single agent gets pushed out of the corridor in an unrealistic manner.

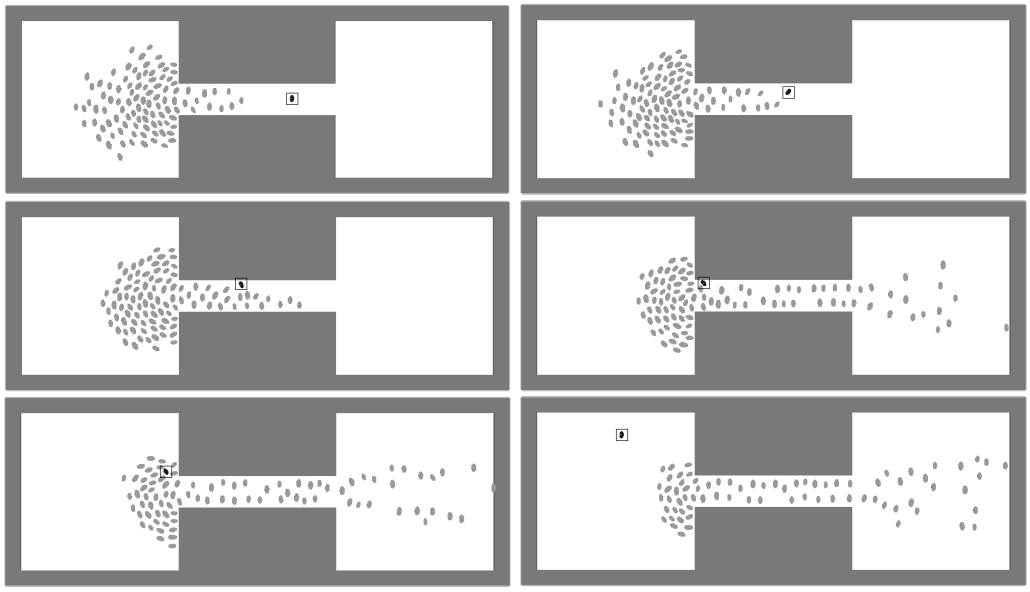

Figure 9: Simulation snapshots using the counterflow model. The single agent is black and highlighted with a square. In this simulation, the single agent is able to pass the crowd in about 25 seconds.

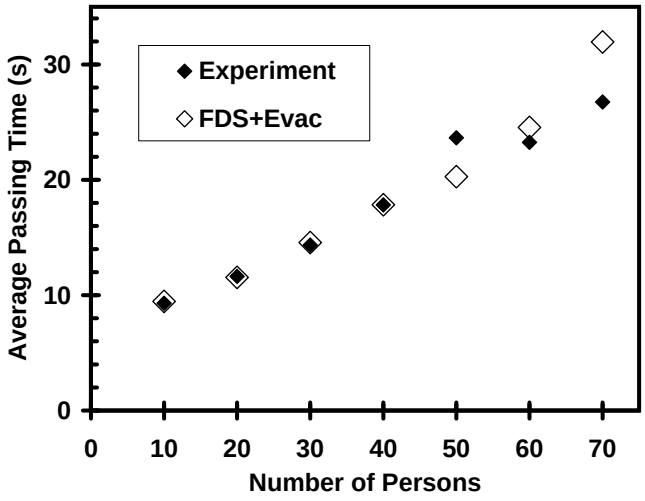

Figure 10: The experimental results of Isobe et al. [35] and simulation results of FDS+Evac with the counterflow model. The values of the simulation results are averages of ten simulation runs.

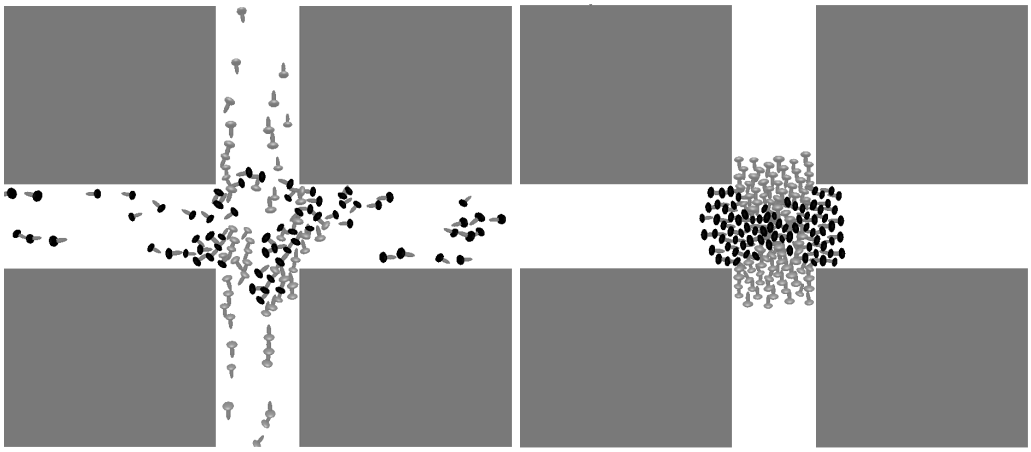

Figure 11: Snapshots of simulations in the crossing. In the left hand figure the collision avoidance model is used, while the right hand one is with the original model. The black agents are moving horizontally and the gray ones vertically. The gray arrow in each agent denotes its moving direction.

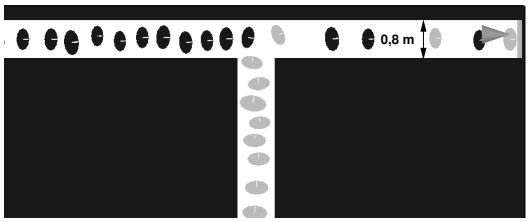

Figure 12: The setting of the first test case for merging flows.

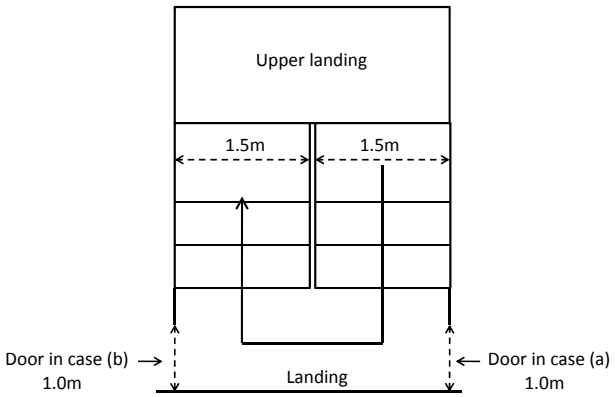

Figure 13: The geometries for test cases (a) and (b) for merging flows in stairs. The big arrow describes the route of the agents walking down the staircase. Depending on the test case, the other stream of agents enters the staircase through either of the two doors and merges into the stair stream.